

Classical optimization with imaginary time block encoding on quantum computers: The MaxCut problem

Dawei Zhong*

Department of Physics & Astronomy, University of Southern California, Los Angeles, CA 90089, USA

Akhil Francis†

*Applied Mathematics and Computational Research Division,
Lawrence Berkeley National Laboratory, Berkeley, CA 94720, USA*

Ermal Rrapaj‡

*Lawrence Berkeley National Laboratory, Berkeley, CA, 94720, USA
Department of Physics, University of California, Berkeley, CA 94720, USA and
RIKEN iTHEMS, Wako, Saitama 351-0198, Japan*

(Dated: November 19, 2024)

Finding ground state solutions of diagonal Hamiltonians is relevant for both theoretical as well as practical problems of interest in many domains such as finance, physics and computer science. These problems are typically very hard to tackle by classical computing and quantum computing could help in speeding up computations and efficiently tackling larger problems. Here we use imaginary time evolution through a new block encoding scheme to obtain the ground state of such problems and apply our method to MaxCut as an illustration. Our method, which for simplicity we call ITE-BE, requires no variational parameter optimization as all the parameters in the procedure are expressed as analytical functions of the couplings of the Hamiltonian. We demonstrate that our method can be successfully combined with other quantum algorithms such as quantum approximate optimization algorithm (QAOA). We find that the QAOA ansatz increases the post-selection success of ITE-BE, and shallow QAOA circuits, when boosted with ITE-BE, achieve better performance than deeper QAOA circuits. For the special case of the transverse initial state, we adapt our block encoding scheme to allow for a deterministic application of the first layer of the circuit.

I. INTRODUCTION

The advent of quantum computers has spurred a wide range of research into quantum advantage: problems that can be solved much faster, and/or at a much larger scale through quantum computing. Some of the most well known cases are integer prime factorization [1], and unstructured search [2], to name a few. An interesting venue of research is discrete optimization problems. These problems can be expressed as the minimization of a polynomial function of binary variables, and the cost function can be written as a diagonal Hamiltonian which encodes the optimal solution in the ground state [3, 4]. For instance, Quadratic Unconstrained Binary Optimization (QUBO) models several problems such as MaxCut, minimum vertex cover, and graph coloring [5, 6]. These problems have found applications in industry [7, 8], condensed matter physics [9], and beyond.

Apart from special cases, finding the exact ground state of such diagonal Hamiltonians is usually difficult, and generally NP-hard [3, 4]. Often heuristic and approximate methods, such as simulated annealing [10] or semidefinite programming [11], are used to approximate solutions classically.

Quantum computers could potentially find solutions beyond the realm of classical computation [12] as quantum hardware moves beyond the noisy intermediate-scale quantum (NISQ) era to fault tolerant computing [13]. Many quantum algorithms such as quantum approximate optimization algorithm (QAOA) [14–18], adiabatic evolution [19], or imaginary time evolution methods [20–23] have been proposed to help determine the ground state. All these methods have their own drawbacks too, such as barren plateaus [24, 25] and other optimization related issues for QAOA [26], longer depth circuits for implementing adiabatic evolution [27] and larger number of measurements for successful post-selection of block encoded implementation of imaginary time evolution [28].

QAOA has been widely explored recently in large sparse graph, and spin glasses [29], in particular in Sherrington-Kirkpatrick (SK) model of spin glass [30], on Maxcut problems [31] in both software and hardware [32–34]. In addition to two-body interactions, QAOA has also been applied to four-body interactions, such as the low autocorrelation binary sequences (LABS) problem [8].

Imaginary time evolution, when applied to an initial state with non-zero overlap with the ground state, exponentially improves the overlap towards the ground state. Since it is a non-unitary operation, implementing it on a quantum computer is not trivial, and there has been several approaches in the literature. One approach is to find equivalent unitary evolutions, with appropriate quantum measurements and classical computations, such

* daweiz@usc.edu

† afrancis@lbl.gov

‡ ermallerapaj@lbl.gov

as in variational imaginary time evolution [20, 35] where a fixed ansatz is updated to follow McLachlan's variational principle. Another approach discretizes the imaginary time evolution and approximates each step by a unitary constructed through tomography [21, 36, 37]. These methods require classical processing and multiple measurements during the time evolution which scale with both system and length of time. Other methods such as block-encoding schemes [38–40], encode the desired non-unitary operation in a bigger unitary matrix, which can then be implemented with ancilla qubits and post-selection. Recently an exact block-encoding scheme for discretized imaginary time evolution, based on unitary Restricted Boltzmann Machines (RBM), has been proposed [28] (for similar recent implementations see [23]).

Here we utilize this imaginary time evolution block encoding (ITE-BE) scheme of the first order Trotter decomposition, to implement imaginary time evolution in solving classical optimization problems such as MaxCut. We also implement a new parametrization that allows to correct for failed post-selection when the initial state is in the traverse state. We find that ITE-BE is beneficial in providing solutions to MaxCut, and also as boosting technique to improve other methods such as QAOA. In Sec. II we define the MaxCut problem, QAOA and the block encoding method ITE-BE. Then, we proceed to perform numerical evaluations of these methods in Sec. III. In Sec. IV we summarize our findings and discuss their implications.

II. PRELIMINARY

A. The MaxCut Problem Definition

In this work, we focus on the MaxCut problem for a given undirected graph $G = (V, \tilde{E})$, where $V = \{1, \dots, N\}$ represents the set of vertices, and $\tilde{E} = \{(\langle j, k \rangle, w_{jk})\}$ denotes the set of edges with non-negative weights $w_{jk} \geq 0$ associated with the edge connecting vertices j and k . The objective of this problem is to partition vertices of graph G into two disjoint subsets such that the sum of weights of the edges linking the two subsets is maximized.

To solve the MaxCut problem, one approach is to formulate it as an integer quadratic programming problem, where the goal is to find a solution $\vec{s} \in \{-1, +1\}^N$ that maximizes the cost function

$$C(\vec{s}) = \frac{1}{2} \sum_{\langle j, k \rangle \in \tilde{E}} w_{jk} (1 - s_j s_k). \quad (1)$$

Here, the solution \vec{s} defines a partition of the graph G , with each node j is labeled by $s_j \in \{-1, +1\}$ indicating which of the two subsets it belongs to. Approximation algorithms, such as the Goemans-Williamson algorithm [11], are employed to find near-optimal solutions efficiently. The Goemans-Williamson algorithm gives the

highest known approximation ratio of $r \approx 0.87856$ among all other classical algorithms for generic graphs [11], while the bound becomes $r \approx 0.9326$ for u3R graphs [41], where $r = C(\vec{s})/C_{\max}$ and C_{\max} is the maximum total cost of the cut.

However, it is NP-hard to design a classical algorithm that achieves $r \geq 16/17$ for MaxCut on all graphs [42]. This limitation motivates the exploration of quantum computing-based methods for solving the MaxCut problem, which are designed to maximize the quantum cost function $-\langle H_C \rangle$. The diagonal Hamiltonian H_C for the MaxCut problem on graph G is given by

$$H_C = - \sum_{\langle j, k \rangle \in \tilde{E}} \frac{w_{jk}}{2} (I - Z_j Z_k), \quad (2)$$

where I is identity operator for N qubit Hilbert space, Z_j and Z_k are Pauli-Z operators acting on qubits corresponding to vertices j and k . Ideally, we expect the quantum algorithm to return a quantum state $|\psi\rangle$ as a superposition of computational basis $|\vec{z}\rangle$, where $\vec{z} \in \{0, 1\}^N$ is a binary string representing a solution of the problem. In this context, each state $|\vec{z}\rangle$ is an eigenvector of $Z_j Z_k$ with eigenvalue ± 1 for any edge $\langle j, k \rangle$, and the quantum cost function $C(\vec{z}) = -\langle \vec{z} | H_C | \vec{z} \rangle$ has a similar structure to the classical cost function $C(\vec{s})$ in the integer quadratic programming problem.

B. Quantum Approximate Optimization Algorithm

The Quantum Approximate Optimization Algorithm (QAOA) is a parameterized quantum algorithm designed to tackle general combinatorial optimization problems, including MaxCut. A p -level QAOA utilizes two parameterized unitary operators, $U(\gamma) = e^{-i\gamma H_C}$ and $U(\beta) = e^{-i\beta H_B}$, to construct a wavefunction for the graph $G = (V, E)$,

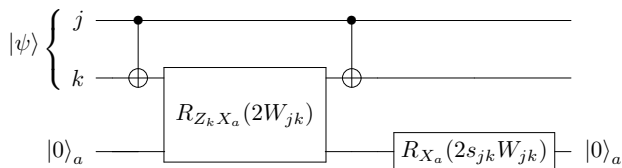
$$|\psi(\vec{\beta}, \vec{\gamma})\rangle = e^{-i\beta_p H_B} e^{-i\gamma_p H_C} \dots e^{-i\beta_1 H_B} e^{-i\gamma_1 H_C} |+\rangle^{\otimes N}. \quad (3)$$

Here, $H_B = \sum_{j=1}^N X_j$ is called the mixing Hamiltonian, where X_j are Pauli- X operators acting on qubit j . The expectation value of H_C can be obtained by repeated measurements of the quantum system in the computational basis,

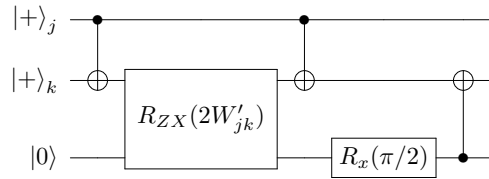
$$\langle H_C(\vec{\beta}, \vec{\gamma}) \rangle = \langle \psi(\vec{\beta}, \vec{\gamma}) | H_C | \psi(\vec{\beta}, \vec{\gamma}) \rangle = \sum_{\vec{z}} \text{Pr}(\vec{z}) \langle \vec{z} | H_C | \vec{z} \rangle, \quad (4)$$

where $\text{Pr}(\vec{z})$ is the probability of measuring the computational basis state $|\vec{z}\rangle$.

To find the optimal parameters $(\vec{\beta}, \vec{\gamma})$, one typically starts from an initial guess and then performs numerical optimization to maximize $\langle H_C(\vec{\beta}, \vec{\gamma}) \rangle$ using feedback from the quantum computer. This iterative process continues until the maximum cost function value is found. A good choice of initial parameters can significantly reduce



(a) RBM inspired block encoding requires post-selection of the ancillary qubit on $|0\rangle$.



(b) Conditional operation based on the ancilla qubit for the physical initial state $|+\rangle_j \otimes |+\rangle_k$ removes the need for post-selection.

FIG. 1: Block-encoding-based circuit implementations for the imaginary-time propagator $e^{-\tau w_{jk} Z_j Z_k / 2}$ with (a) a generic input state $|\psi\rangle$ and (b) the input state $|+\rangle_j \otimes |+\rangle_k$. Circuit parameters are given in eq. 8 and eq. A4. These block encodings can be applied for a generic Pauli string propagator $e^{-K \prod_i \sigma_i}$.

the computational cost of optimization. Heuristic strategies have been proposed to optimize $\langle H_C(\vec{\beta}, \vec{\gamma}) \rangle$ with respect to parameters $(\vec{\beta}, \vec{\gamma})$ using a good initial guess [33].

Recently, Ref. [29, 30] applied QAOA to the Sherrington-Kirkpatrick (SK) model and derived near-optimal parameters $(\vec{\beta}, \vec{\gamma})$ for $p < 20$, and at $p = 11$ they find that QAOA outperforms the standard semi-definite programming algorithm.

C. ITE-BE Method

Imaginary-time evolution (ITE) is a widely used approach to determine the ground state of a Hamiltonian H , by evolving the quantum system through the imaginary-time propagator

$$|\psi(\tau)\rangle = e^{-\tau H} |\psi(0)\rangle, \tau > 0. \quad (5)$$

As long as the initial state $|\psi(0)\rangle$ is not orthogonal to the ground state and τ is sufficiently large.

The ITE method can also be applied to classical optimization problems if the classical cost function can be expressed as the expectation value of a problem Hamiltonian. For example, the ITE method can solve the MaxCut problem by finding ground states of Hamiltonian H_C , which maximize the MaxCut cost function. In this case, the imaginary-time propagator is given by

$$e^{-\tau H_C} = e^{\tau \sum_{\langle j,k \rangle} \frac{w_{jk}}{2} I} e^{-\tau \sum_{\langle j,k \rangle} \frac{w_{jk}}{2} Z_j Z_k}. \quad (6)$$

Here, $e^{\tau \sum_{\langle j,k \rangle} \frac{w_{jk}}{2} I}$ is a global phase factor that can be ignored, and the second term can be exactly decomposed as

$$e^{-\tau \sum_{\langle j,k \rangle} \frac{w_{jk}}{2} Z_j Z_k} = \prod_{\langle j,k \rangle} e^{-\tau \frac{w_{jk}}{2} Z_j Z_k}, \quad (7)$$

which does not incur Trotter error because all $Z_j Z_k$ operators in the sum on the left-hand side commute with each other. Therefore, we can choose a sufficiently large time step τ to ensure convergence. Since each term on the

right-hand side is non-unitary, we implement them using a block-encoding-based method proposed in Ref. [28]. The circuit block for $e^{-\tau \frac{w_{jk}}{2} Z_j Z_k}$ is shown in Fig. 1a, and the parameters in the circuit block can be determined analytically by

$$\begin{aligned} W_{jk} &= \frac{1}{2} \cos^{-1} [\exp(-|\tau w_{jk}|)], \\ s_{jk} &= \text{sign}(W_{jk}). \end{aligned} \quad (8)$$

In this approach, data will be discarded unless the ancilla qubit is measured to be $|0\rangle$. If the input state to a certain circuit block is $|+\rangle_j \otimes |+\rangle_k$, we can modify the block encoding parameters to deterministically apply the imaginary time propagator, see Fig. 1b. We refer readers to Appendix A for further details.

III. PROTOCOLS AND EVALUATION

In this section, we design two protocols built upon the imaginary-time evolution to solve the MaxCut problem. The first protocol is a purely ITE-BE method starting with initial state $|+\rangle^{\otimes N}$, in which we adopt the circuit shown in Fig. 1b for the first layer and apply the circuit in Fig. 1a for the subsequent layers. This choice improves the post-selection rate by effectively setting to 1 for the first layer, even when the ancilla is not measured to be $|0\rangle$ state. The second protocol starts with the QAOA circuit, followed by ITE-BE, see Fig. 2. In essence, this method uses a QAOA circuit to prepare an initial state with a non-minimal overlap with the ground state. Then, the state is evolved through ITE-BE to significantly enhance the overlap.

Both methods can be applied to general settings. As proof of concept, we numerically evaluate the performance of these protocols on unweighted 3-regular (u3R) graphs with vertex number $6 \leq N \leq 12$. We finally report the 99.7% uncertainty intervals for approximation ratio r , the probability of obtaining the optimal solution $p_{\text{opt}} = N_{\text{opt}}/N_{\text{tot}}$ and the post-selection rate. Here, N_{tot}

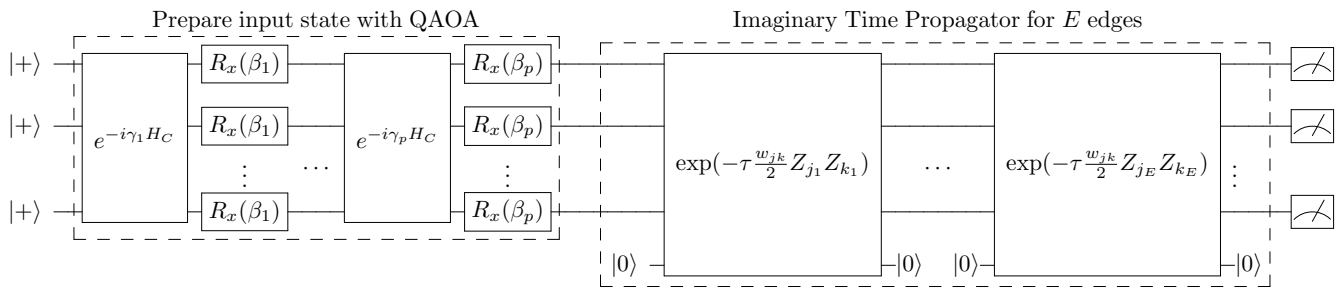


FIG. 2: The protocol of QAOA+ITE-BE method with a p -level QAOA circuit state preparation for ITE-BE rather than using the equal superposition state $|+\rangle^{\otimes n}$.

is the number of measurements made on data qubits after the post-selection of the ITE-BE method, and N_{opt} is the number of times one of the optimal solutions is obtained. Both metrics estimate the average quality of an algorithm, but p_{opt} is more conservative because it directly reflects the algorithm's ability to find exact solutions. The post-selection rate denotes the success rate of the block encoding procedure, which is the probability in getting all $|0\rangle$ state for the ancilla qubits.

A. ITE-BE Only

Our first method is purely based on the imaginary time evolution. Since all $Z_j Z_k$ terms commute in the sum on the left-hand side of Eq. 7, we can rearrange the order of multiplication on the right-hand side of the same equation and separate them into two parts V_1 and V_2 . For the first part, we define $V_1 = \prod_{\langle j,k \rangle} e^{-\tau \frac{w_{jk}}{2} Z_j Z_k}$ using edges $\langle j, k \rangle$ that form a maximal matching in the graph, i.e., a set of disjoint edges without common vertices that includes as many nodes as possible. All imaginary propagators in V_1 can be implemented by the circuit with correction shown in Fig. 1b when the protocol starts with initial state $|+\rangle^{\otimes N}$. The second part consists of all remaining edges in the graph, and they can be only implemented using the circuit in Fig. 1a as the input state of each block is no longer $|+\rangle_j \otimes |+\rangle_k$. We have verified that this choice enhances post-selection success. To reduce the overhead of this approach, ancilla qubits for each block can be reused by performing mid-circuit measurements and resetting them to $|0\rangle$. In this case, the current shot terminates and a new shot begins if any of the ancilla qubits in the second part is measured to be $|1\rangle$. All data qubits are measured only after all circuit blocks for the imaginary time propagator $e^{-\tau H_C}$ have been executed.

We then apply this method to solve the MaxCut problem on 100 randomly generated u3R graph instances with fixed N , where $w_{jk} = 1$ for any j, k in edges E and each node is connected exactly to three other nodes. The imaginary time τ is varied from 0 to 2 which allows us to observe how the results evolve until they are sufficiently close to the ideal solutions. For each τ , we run the

ITE-BE circuit with 10^5 shots for each individual graph and calculate the approximation ratio, the probability of obtaining the optimal solution, and the post-selection success rate using data from successful executions. We repeat this process 10 times to accumulate enough samples and reduce statistical fluctuations. Finally, we exclude graphs with at least one overall failure (i.e., all 10^5 shots discarded) in 10 repetitions, and report 99.7% uncertainty intervals of above three metrics in Fig. 3. For comparison, we also show the bound of approximation ratio $r \approx 0.9326$ of classical semidefinite programming for u3R graphs [41]. All quantum circuits were simulated with the `AerSimulator` backend provided by the `Qiskit` Python package [43].

Our simulation shows that, as expected, both the approximation ratio r and the probability of obtaining optimal solutions p_{opt} increase monotonically with imaginary time τ across all graph sizes and eventually saturate near the optimal value of 1.0 as τ approaches 2. Meanwhile, the post-selection success rate decreases exponentially with τ , which is consistent with the prediction of the success rate in Ref. [28]. We note that smaller graphs converge more quickly to the ground state and exhibit higher post-selection success rates compared to larger graphs due to fewer terms in the Hamiltonian. As the figure shows, $r \geq 0.5$ even at $\tau = 0$ (just the $|+\rangle^{\otimes N}$ state). For further details on why this is the case, see Appendix D.

Further analysis shows that for bipartite graph, the ITE-BE method shows a faster convergence to the ground state and higher success rate compared to non-bipartite graphs of the same size. As a result, we do not consider bipartite graphs in Fig. 3 and provide a detailed investigation of the ITE-BE method on MaxCut problem for them in Appendix B.

B. QAOA + ITE-BE

Our second method combines the QAOA with the imaginary time evolution (see Fig. 2). In the first part of the protocol, instead of training QAOA for parameter $(\vec{\beta}, \vec{\gamma})$, we adopt near-optimal values from Ref. [29]

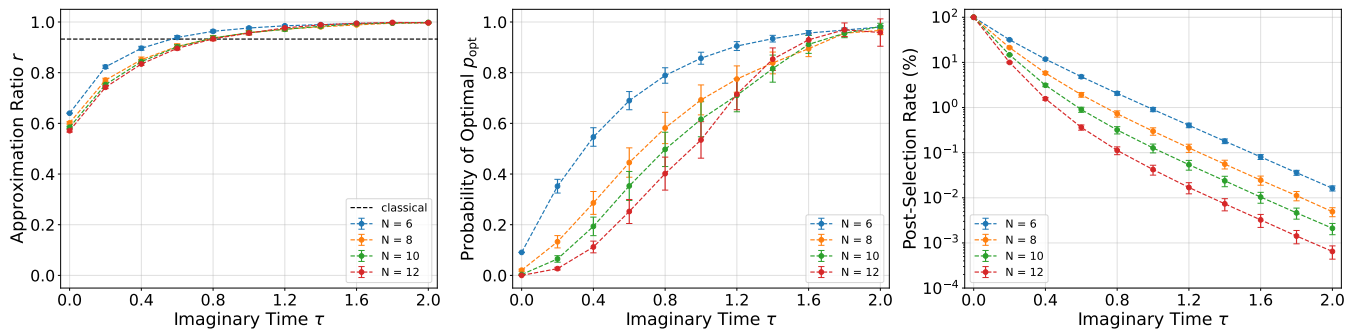


FIG. 3: The averaged approximation ratio r , probability of obtaining optimal solution p_{opt} , and the post-selection success rate for randomly generated unweighed 3-regular graphs within three standard deviations of the mean for ITE-BE method. This method guarantees convergence to the optimal solution, while the post-selection success rate decays exponentially. The convergence becomes slower and the success rate decreases when the problem size N increases.

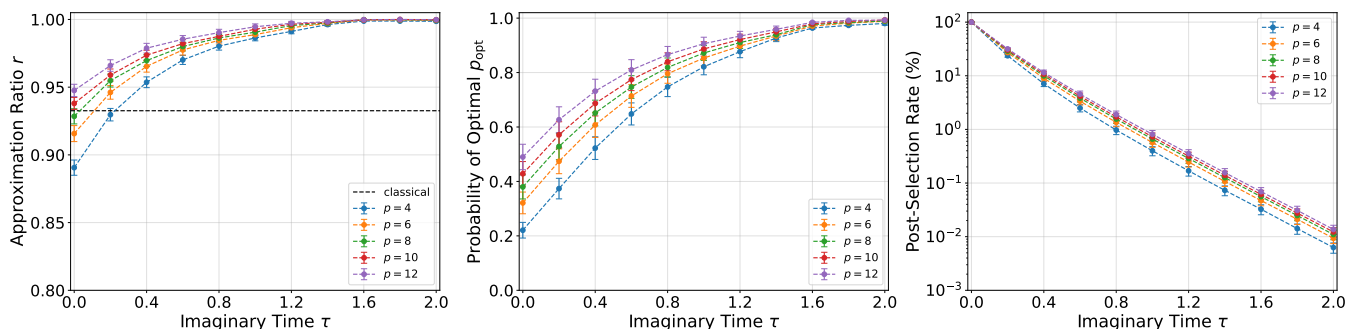


FIG. 4: The averaged approximation ratio r , probability of obtaining optimal solution p_{opt} , and the post-selection success rate within three standard deviations of the mean for the QAOA+ITE-BE method. Here we use p -level QAOA circuit for state preparation, where $p = 4, 6, 8, 10, 12$. The QAOA input state leads to faster convergence of ITE-BE and a post-selection rate that is one order of magnitude higher than using an equal superposition state to solve same graph for $p = 12$.

and prepare the input state using a p -level QAOA circuit. The QAOA output state has a higher overlap with the ground state than the standard equal superposition state $|+\rangle^{\otimes n}$. As such we expect this protocol to improve the post-selection success rate in the subsequent ITE-BE part. In the second part, we apply the ITE-BE method to further search for the optimal solution, where each imaginary time propagator for edge (j, k) is implemented by the circuit block in Fig. 1a. To reduce the resource overhead of the ITE-BE part, we reuse ancilla qubits for each circuit block by mid-circuit measurement and reset as in the pure ITE-BE method. The data qubits are measured only after all circuit blocks have been executed.

In order to evaluate its performance, we apply this hybrid approach to solve the MaxCut problem on the same set of randomly generated unweight 3-regular(u3R) graph instances as in Sec. III A, following the same settings. We report the 99.7% averaged uncertainty interval for the averaged approximation ratio r , probability of optimal p_{opt} and post-selection success rate as a function of imaginary time τ for graphs with $N = 12$ and differ-

ent QAOA levels in Fig. 4. The black dashed line is the classical bound of approximation ratio $r \approx 0.9326$.

Similar to the pure ITE-BE results, both r and p_{opt} increase monotonically with time τ , and the final results always converge to the ground state at $\tau \sim 2$ regardless of the QAOA level. Also, the post-selection success rate decays exponentially with τ , but this trend is independent on the QAOA level. These observations suggest that a shallow QAOA+ITE-BE circuit with a lower p and a large τ is sufficient to obtain the optimal solution. Additional results for graphs with $N = 6, 8, 10$ lead to the same conclusion, and the data can be found in Appendix C. For bipartite graphs, this method demonstrates rapid convergence and high success rate which eventually reach a plateau. We do not consider bipartite graphs in Fig. 4, but study the performance on Appendix B.

It is worth noting that at $\tau = 0$, the imaginary time propagator does not act on the input state. Thus, the values of both r and p_{opt} at $\tau = 0$ reflect the performance of p -level QAOA with near-optimal parameter

values from Ref. [29]. As shown in Fig. 4, the QAOA output state achieves a higher approximation ratio but a lower probability of obtaining optimal solution. This behavior indicates that the QAOA output state is a superposition of the ground state and multiple excited state, $|\psi\rangle = \sum_j c_j |\bar{z}_j\rangle$. The presence of excited states lead to a lower p_{opt} , but their total contribution to the cost function $\langle H_C \rangle$ is significantly smaller than that of the ground state, which results in a high approximation ratio. We can conclude that parameter values in Ref. [29] are tuned to maximize r rather than p_{opt} , and the ITE-BE layer significantly enhance performance of QAOA to achieve a higher p_{opt} while also improving r .

Another interesting comparison can be made on the post-selection rate as function of the initial state. Not only does the ITE-BE method improve the results of QAOA, but also the initial state provided by QAOA increases the post-selection rate with respect to the $|+\rangle^{\otimes n}$. Indeed, for $\tau = 2$ and $N = 12$ the post-selection rate increases by about an order of magnitude.

IV. CONCLUSION AND OUTLOOK

In this paper, we propose two quantum algorithms based on the block-encoding implementation of the imaginary time evolution propagator (ITE-BE) and evaluate their performance on the MaxCut problem. We note that ITE-BE requires no parameter optimization and can be applied to any Pauli string Hamiltonian, see Fig. 1 for illustrations. We conduct numerical simulations on randomly generated unweight 3-regular graphs with vertex number from $N = 6$ to $N = 12$. Our result shows that both ITE-BE based methods guarantee convergence to the ground state when the imaginary time τ is sufficiently large, and the ITE-BE based methods are promising to solve combinatorial optimization problems with high accuracy at the cost of larger number of shots due to post-selection requirements.

The success of QAOA+ITE-BE method emphasizes the importance of concatenating quantum algorithms in order to boost overall performance and overcome individual limitations. When preparing the initial state with a p -level QAOA for the ITE-BE layer, our results show

a faster convergence of ITE-BE to the optimal solution and a post-selection rate that is an order of magnitude higher than using $|+\rangle^{\otimes n}$ as initial state. The result of QAOA+ITE-BE also reveals a trade-off between the QAOA level p and the imaginary time τ , namely, one can choose a lower QAOA level with a large τ to ensure convergence using a shallow circuit, or choose higher QAOA level to have quicker convergence with higher post-selection rate. Moreover, integrating QAOA with the ITE-BE method also benefits QAOA, as it avoids the need for additional training of QAOA with near-optimal parameters to achieve better accuracy. Instead, the subsequent ITE-BE layer enhances the result with only $O(E)$ circuit depth, where E is the number of edges in the graph. This improvement is particularly significant when solving MaxCut on large graphs.

Our work focuses mainly on the MaxCut problem, but the principle of both the ITE-BE and QAOA+ITE-BE methods can be applied to other combinatorial optimization problems such as the traveling Salesman problem or the Knapsack problem. The practical application of these methods is limited by the exponential decay in post-selection success rates with increasing imaginary time τ and graph size N . Therefore, developing methods to improve the post-selection success rate or enhance the convergence speed is a crucial research direction we leave for exploration in future work. By solving this challenge with advanced algorithm designs, we will be able to realize the full potential of imaginary time evolution on optimization problems and achieve practical quantum advantage.

V. ACKNOWLEDGMENT

A.F. acknowledges funding by the U.S. Department of Energy, Office of Science, Office of Advanced Scientific Computing Research Quantum Testbed Program under contract DE-AC02-05CH11231. The authors acknowledge the Center for Advanced Research Computing (CARC) at the University of Southern California for providing computing resources that have contributed to the research results reported within this publication. URL: <https://carc.usc.edu>.

-
- [1] P. Shor, Algorithms for quantum computation: discrete logarithms and factoring, in *Proceedings 35th Annual Symposium on Foundations of Computer Science* (1994) pp. 124–134.
 - [2] L. K. Grover, Quantum mechanics helps in searching for a needle in a haystack, *Phys. Rev. Lett.* **79**, 325 (1997).
 - [3] F. Barahona, On the computational complexity of ising spin glass models, *Journal of Physics A: Mathematical and General* **15**, 3241 (1982).
 - [4] A. Lucas, Ising formulations of many np problems, *Frontiers in Physics* **2**, 10.3389/fphy.2014.00005 (2014).
 - [5] G. Kochenberger, J.-K. Hao, F. Glover, M. Lewis, Z. Lü, H. Wang, and Y. Wang, The unconstrained binary quadratic programming problem: a survey, *Journal of Combinatorial Optimization* **28**, 58 (2014).
 - [6] A. Mazumder and S. Tayur, Five starter problems: Solving quadratic unconstrained binary optimization models on quantum computers (2024), [arXiv:2401.08989](https://arxiv.org/abs/2401.08989) [quant-ph].
 - [7] M. Streif, S. Yarkoni, A. Skolik, F. Neukart, and M. Leib, Beating classical heuristics for the binary paint shop problem with the quantum approximate optimization al-

- gorithm, *Phys. Rev. A* **104**, 012403 (2021).
- [8] R. Shaydulin, C. Li, *et al.*, Evidence of scaling advantage for the quantum approximate optimization algorithm on a classically intractable problem, *Science Advances* **10**, eadm6761 (2024).
- [9] M. Mezard, G. Parisi, and M. Virasoro, *Spin Glass Theory and Beyond* (WORLD SCIENTIFIC, 1986).
- [10] S. Kirkpatrick, C. D. Gelatt, and M. P. Vecchi, Optimization by simulated annealing, *Science* **220**, 671 (1983).
- [11] M. X. Goemans and D. P. Williamson, Improved approximation algorithms for maximum cut and satisfiability problems using semidefinite programming, *J. ACM* **42**, 1115–1145 (1995).
- [12] A. Abbas *et al.*, Challenges and opportunities in quantum optimization, *Nature Reviews Physics* **10.1038/s42254-024-00770-9** (2024).
- [13] P. C. Lotshaw *et al.*, Scaling quantum approximate optimization on near-term hardware, *Scientific Reports* **12**, 12388 (2022).
- [14] E. Farhi, J. Goldstone, and S. Gutmann, A quantum approximate optimization algorithm (2014), [arXiv:1411.4028 \[quant-ph\]](https://arxiv.org/abs/1411.4028).
- [15] E. Farhi and A. W. Harrow, Quantum supremacy through the quantum approximate optimization algorithm (2019), [arXiv:1602.07674 \[quant-ph\]](https://arxiv.org/abs/1602.07674).
- [16] S. Lloyd, Quantum approximate optimization is computationally universal (2018), [arXiv:1812.11075 \[quant-ph\]](https://arxiv.org/abs/1812.11075).
- [17] E. Farhi, J. Goldstone, S. Gutmann, and H. Neven, Quantum algorithms for fixed qubit architectures (2017), [arXiv:1703.06199 \[quant-ph\]](https://arxiv.org/abs/1703.06199).
- [18] D. Wecker, M. B. Hastings, and M. Troyer, Training a quantum optimizer, *Phys. Rev. A* **94**, 022309 (2016).
- [19] E. Farhi, J. Goldstone, S. Gutmann, J. Lapan, A. Lundgren, and D. Preda, A quantum adiabatic evolution algorithm applied to random instances of an np-complete problem, *Science* **292**, 472 (2001).
- [20] S. McArdle *et al.*, Variational ansatz-based quantum simulation of imaginary time evolution, *npj Quantum Information* **5**, 75 (2019).
- [21] M. Motta, C. Sun, A. T. K. Tan, M. J. O’Rourke, E. Ye, A. J. Minnich, F. G. S. L. Brandão, and G. K.-L. Chan, Determining eigenstates and thermal states on a quantum computer using quantum imaginary time evolution, *Nature Physics* **16**, 205 (2020).
- [22] Y. Huang, Y. Shao, W. Ren, J. Sun, and D. Lv, Efficient quantum imaginary time evolution by drifting real-time evolution: An approach with low gate and measurement complexity, *Journal of Chemical Theory and Computation* **19**, 3868 (2023).
- [23] C. Leadbeater, N. Fitzpatrick, D. M. Ramo, and A. J. W. Thom, Non-unitary trotter circuits for imaginary time evolution, *Quantum Science and Technology* **9**, 045007 (2024).
- [24] S. Wang *et al.*, Noise-induced barren plateaus in variational quantum algorithms, *Nature Communications* **12**, 6961 (2021).
- [25] Z. Holmes, K. Sharma, M. Cerezo, and P. J. Coles, Connecting ansatz expressibility to gradient magnitudes and barren plateaus, *PRX Quantum* **3**, 010313 (2022).
- [26] L. Bittel and M. Kliesch, Training variational quantum algorithms is np-hard, *Phys. Rev. Lett.* **127**, 120502 (2021).
- [27] W. van Dam, M. Mosca, and U. Vazirani, How powerful is adiabatic quantum computation?, in *Proceedings 42nd IEEE Symposium on Foundations of Computer Science* (2001) pp. 279–287.
- [28] E. Rrapaj and E. Rule, Exact block encoding of imaginary time evolution with universal quantum neural networks (2024), [arXiv:2403.17273 \[quant-ph\]](https://arxiv.org/abs/2403.17273).
- [29] J. Basso, D. Gamarnik, S. Mei, and L. Zhou, Performance and limitations of the qaoa at constant levels on large sparse hypergraphs and spin glass models, in *2022 IEEE 63rd Annual Symposium on Foundations of Computer Science (FOCS)* (2022) pp. 335–343.
- [30] E. Farhi, J. Goldstone, S. Gutmann, and L. Zhou, The Quantum Approximate Optimization Algorithm and the Sherrington-Kirkpatrick Model at Infinite Size, *Quantum* **6**, 759 (2022).
- [31] G. E. Crooks, Performance of the quantum approximate optimization algorithm on the maximum cut problem (2018), [arXiv:1811.08419 \[quant-ph\]](https://arxiv.org/abs/1811.08419).
- [32] R. Shaydulin and M. Pistoia, Qaoawith $n \cdot p \geq 200$, in *2023 IEEE International Conference on Quantum Computing and Engineering (QCE)*, Vol. 01 (2023) pp. 1074–1077.
- [33] L. Zhou, S.-T. Wang, S. Choi, H. Pichler, and M. D. Lukin, Quantum approximate optimization algorithm: Performance, mechanism, and implementation on near-term devices, *Phys. Rev. X* **10**, 021067 (2020).
- [34] M. P. Harrigan *et al.*, Quantum approximate optimization of non-planar graph problems on a planar superconducting processor, *Nature Physics* **17**, 332 (2021).
- [35] J. Gacon *et al.*, Variational quantum time evolution without the quantum geometric tensor, *Phys. Rev. Res.* **6**, 013143 (2024).
- [36] Y. Huang *et al.*, Efficient quantum imaginary time evolution by drifting real-time evolution: An approach with low gate and measurement complexity, *Journal of Chemical Theory and Computation* **19**, 3868 (2023).
- [37] F. Turro, A. Roggero, V. Amitrano, P. Luchi, K. A. Wendt, J. L. Dubois, S. Quaglioni, and F. Pederiva, Imaginary-time propagation on a quantum chip, *Phys. Rev. A* **105**, 022440 (2022).
- [38] A. M. Childs and N. Wiebe, Hamiltonian simulation using linear combinations of unitary operations, *Quantum Info. Comput.* **12**, 901–924 (2012).
- [39] G. H. Low and I. L. Chuang, Optimal hamiltonian simulation by quantum signal processing, *Phys. Rev. Lett.* **118**, 010501 (2017).
- [40] A. Gilyén, Y. Su, G. H. Low, and N. Wiebe, Quantum singular value transformation and beyond: exponential improvements for quantum matrix arithmetics, in *Proceedings of the 51st Annual ACM SIGACT Symposium on Theory of Computing* (2019) p. 193–204.
- [41] E. Halperin, D. Livnat, and U. Zwick, Max cut in cubic graphs, *Journal of Algorithms* **53**, 169 (2004).
- [42] J. Håstad, Some optimal inapproximability results, *J. ACM* **48**, 798–859 (2001).
- [43] A. Javadi-Abhari *et al.*, Quantum computing with qiskit (2024), [arXiv:2405.08810 \[quant-ph\]](https://arxiv.org/abs/2405.08810).

Appendix A: ITE Parameters

We provide here the general form of the ansatz for a single qubit (the same analysis applies to n-qubit Pauli string),

$$e^{-\tau K \sigma_r} = \mathcal{N} \langle 0_a | e^{-i(c\sigma_a^x + W\sigma_r\sigma_a^x)} | 0_a \rangle, \quad (\text{A1})$$

where W is the coupling between ancilla qubit a and the target qubit r . For a generic initial state, $|\Psi\rangle = \alpha|0\rangle + \beta|1\rangle$ with $|\beta|^2 = 1 - |\alpha|^2$, the ratio of the probability to measure $|0_a\rangle$ versus $|1_a\rangle$ is,

$$\frac{P(0_a)}{P(1_a)} = \left| \frac{\alpha \cos(c+W) + \beta \cos(c-W)}{\alpha \sin(c+W) + \beta \sin(c-W)} \right|^2. \quad (\text{A2})$$

In [28], the values of the parameters are,

$$\begin{aligned} \mathcal{N} &= \exp(|\tau K|)/2, \\ W &= \frac{1}{2} \cos^{-1}[\exp(-2|\tau K|)], \\ c &= Ws, \quad s = \text{sign}(K). \end{aligned} \quad (\text{A3})$$

When post-selection fails, one must repeat the operation. However, for special cases, one can correct instead of re-starting computations. For instance, instead of the parameters in the (A3), we can use the following parameters,

$$\begin{aligned} \mathcal{N} &= \frac{\sqrt{e^{4\tau K} + 1}}{2\sqrt{e^{2\tau K}}}, \\ W &= \tan^{-1}(e^{2\tau K}) - \pi/4, \\ c &= \pi/4. \end{aligned} \quad (\text{A4})$$

The state post operation is,

$$\begin{aligned} U(|\Psi\rangle \otimes |0_a\rangle) &= \frac{1}{\sqrt{e^{4K\tau} + 1}} (\alpha|0\rangle + \beta e^{2K\tau}|1\rangle) \otimes |0_a\rangle \\ &\quad - \frac{ie^{2K\tau}}{\sqrt{e^{4K\tau} + 1}} (\alpha|0\rangle + \beta e^{-2K\tau}|1\rangle) \otimes |1_a\rangle. \end{aligned} \quad (\text{A5})$$

Thus, when the ancilla is measure in the $|0_a\rangle$ state, the desired operation is performed in the system qubit, and when the ancilla is measure in the $|1_a\rangle$ state, the opposite operation is performed. If $\alpha = \beta$, we can flip the amplitudes with a CX gate, effectively correcting post-selection, and no measurement is required. The ancilla can be reset for re-use.

Appendix B: The MaxCut Solution of Bipartite Graphs

During the process of data analysis, we observe that both ITE-BE methods converge more quickly for some graphs than for others in our sample. Moreover, these graphs have higher post-selection success rate compared

to other graph with same size, and the success rate reaches a plateau after a certain imaginary time τ . To understand the conditions under which the ITE-BE method converges more quickly, we compute the spectra of both the adjacency matrices and Hamiltonians of these special graphs. We found that the minimum eigenvalue of the adjacency matrices of these graphs is -3 , which is a characteristic feature of unweighted bipartite 3-regular graphs. In addition, the minimum eigenvalue of their Hamiltonian H_C is given by $(\frac{3N}{2} - 1)/2$, where $\frac{3N}{2}$ is the total number of edges in a 3-regular graph. This implies that the MaxCut solution is a partition where all edges in the graph connect the two parts of the partition. These observations conclusively identify the special graphs as bipartite 3-regular graphs.

To verify whether the ITE-BE method converges quickly on other bipartite 3-regular graphs, we randomly generate 40 instances of bipartite graphs with $6 \leq N \leq 12$ nodes, and solve the MaxCut problem using both ITE-BE and QAOA + ITE-BE methods. The numerical simulation setting and data analysis process are consistent with those described in the main text. The results are shown in Fig. 5 and Fig. 6.

It is worth noting that for any bipartite graph with weights $w_{jk} = 1$, the solution to the MaxCut problem is unique and corresponds to the bipartition of the graph. This is because, in a bipartite graph, all edges connect vertices from one part to the other, so the total weight of the edges crossing the bipartition is maximized and cannot be increased further. In this case, the MaxCut solution can be found using classical algorithms such as breadth-first search (BFS) or depth-first search (DFS) with linear time complexity $O(V + E)$. Therefore, a quantum algorithm cannot achieve exponential speed-up to provide a quantum advantage for MaxCut problem in bipartite graph, but should not perform worse than classical algorithms.

Appendix C: QAOA+ITE-BE Results for Graphs with 6, 8, 10 Nodes

In this appendix, we show the results of the QAOA+ITE-BE method on u3R graph instances with $N = 6, 8$ and 10 in Fig. 7. Due to the optimal parameters for QAOA, at $\tau = 0$, the approximation ratio is already above 0.9 and further improves with ITE-BE. The p_{opt} at $\tau = 0$, on the other hand, is smaller in value and decreases significantly as the system become larger, compared to approximation ratio, for the optimal QAOA. The application of the ITE-BE layer increases the overlap with the ground state, as expected.

Appendix D: Approximation Ratio

Here is an illustration of why the approximation ratio for $|+\rangle^{\otimes n}$ is above 0.5. For an arbitrary state $|\psi\rangle$, the

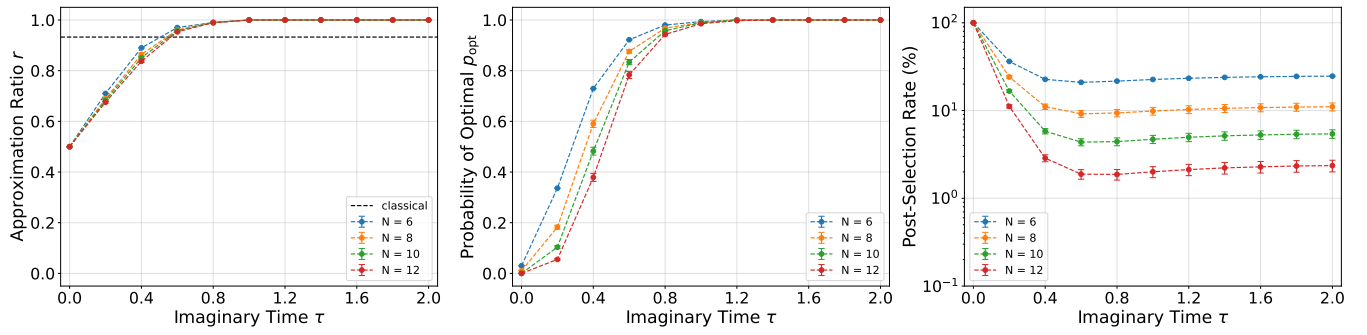


FIG. 5: The averaged performance of pure ITE-BE method on 40 randomly generated bipartite 3-regular graphs for $N = 6, 8, 10$ and 12 . The ITE-BE method converges faster than non-bipartite graphs and the success rate reaches a plateau after imaginary time $\tau \sim 0.6$.

cost function of $\langle H_C \rangle$ where $w_{jk} = 1$ is given by

$$\langle \psi | H_C | \psi \rangle = \frac{1}{2} \sum_{\langle j,k \rangle} (\langle \psi | Z_j Z_k | \psi \rangle - \langle \psi | I | \psi \rangle). \quad (\text{D1})$$

There are totally $3N/2$ edges for a 3-regular graph, so

$$\langle H_C \rangle = \frac{1}{2} \sum_{\langle j,k \rangle} \langle \psi | Z_j Z_k | \psi \rangle - \frac{3N}{4}. \quad (\text{D2})$$

If consider bipartite graph and let $|\phi\rangle = \frac{1}{\sqrt{2^n}} |+\rangle^{\otimes n}$, then the first term $\frac{1}{2} \sum_{\langle j,k \rangle} \langle \psi | Z_j Z_k | \psi \rangle$ is very close to 0, so $\langle H_C \rangle_\phi = \frac{3N}{4}$. The MaxCut for bipartite graph will cut all edges of the graph, so $\langle \psi | Z_j Z_k | \psi \rangle = -1$ for any j, k . Then for optimal solution,

$$\langle H_C \rangle = \frac{1}{2} \sum_{\langle j,k \rangle} (\langle \psi | Z_j Z_k | \psi \rangle) - \frac{3N}{4} = -\frac{3N}{4} - \frac{3N}{4} = -\frac{3N}{2}, \quad (\text{D3})$$

and the approximation ratio for $|\phi\rangle$ on bipartite graph is

$$r = \frac{\langle H_C \rangle_\phi}{\langle H_C \rangle} = 0.5. \quad (\text{D4})$$

For non-bipartite graph, more than one $\langle \psi | Z_j Z_k | \psi \rangle = 1$ in the sum of eq. D2. In this case, the cost function for the MaxCut will still be negative but larger than $-\frac{3N}{2}$, then the approximation ratio for $|\phi\rangle$ on non-bipartite graph is

$$r' = \frac{\langle H_C \rangle_\phi}{\langle H_C \rangle'} \geq \frac{\langle H_C \rangle_\phi}{\langle H_C \rangle} = 0.5. \quad (\text{D5})$$

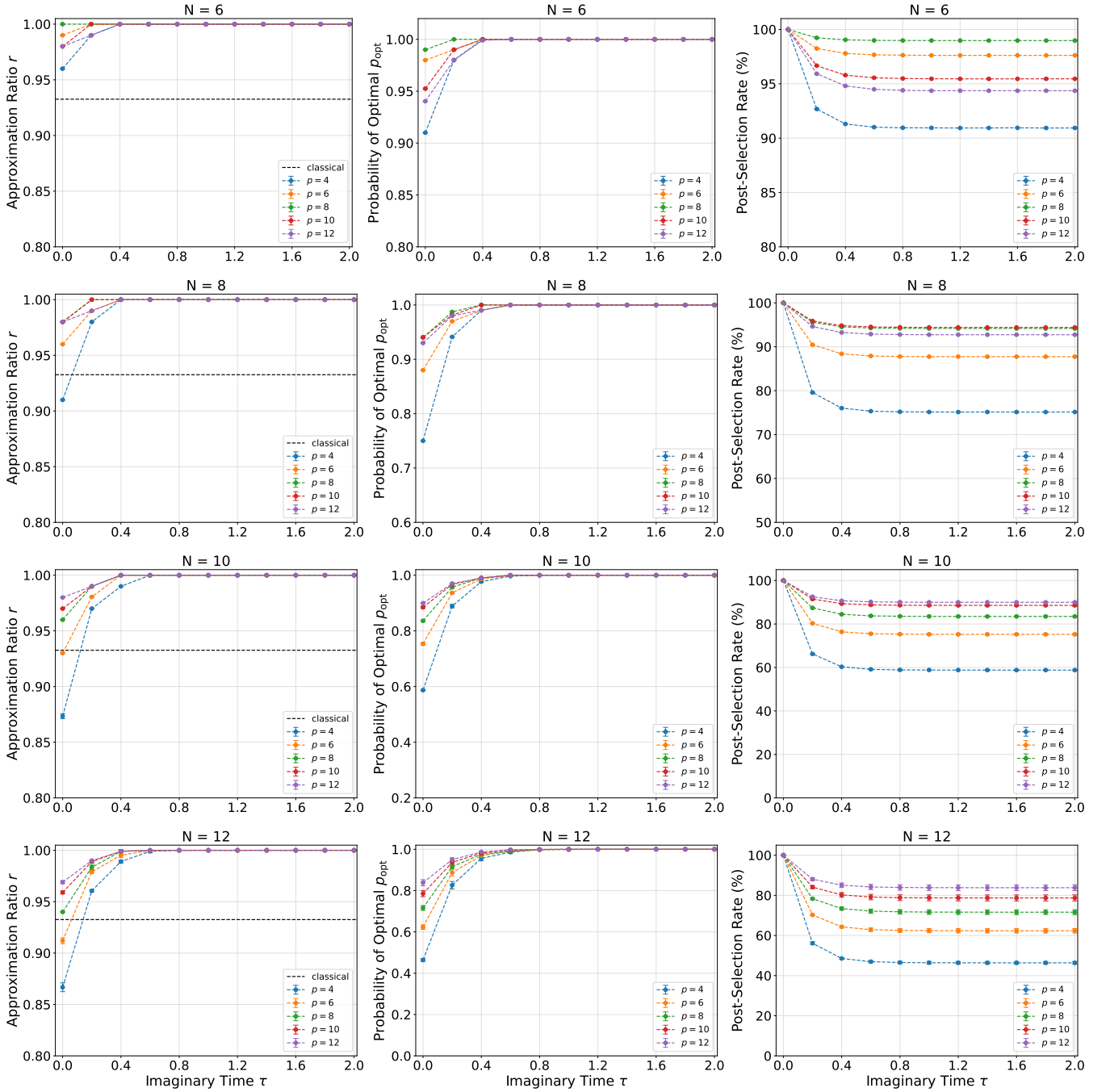


FIG. 6: The averaged performance of QAOA+ITE-BE method on 40 randomly generated bipartite 3-regular graphs for $N = 6, 8, 10$ and 12 . In this case, the QAOA initial state is very close to the optimal solution so the ITE-BE method have only smaller improvement. The success rate reaches a plateau after imaginary time $\tau \sim 0.4$.

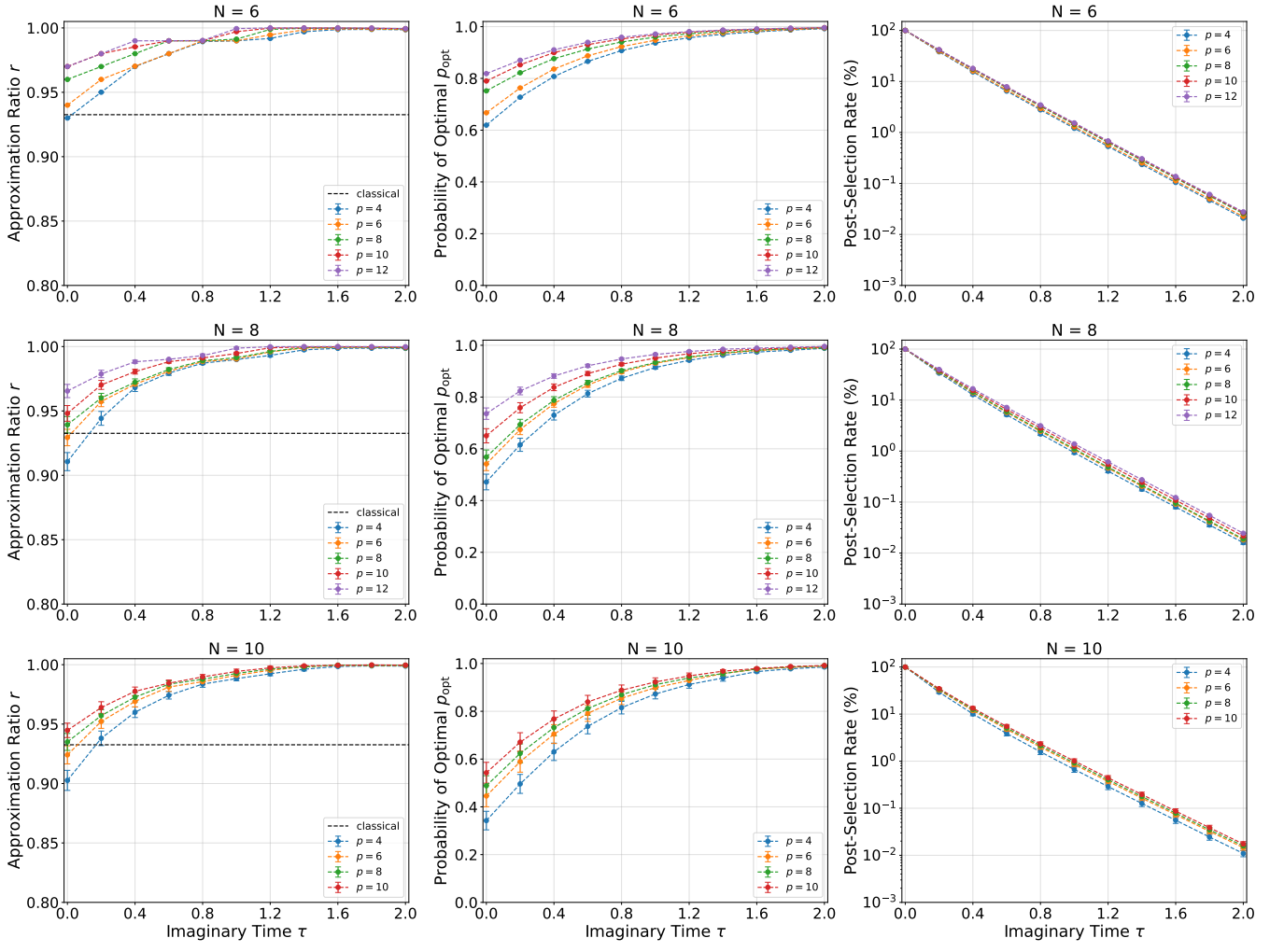


FIG. 7: The averaged performance of QAOA+ITE-BE method on 40 randomly generated bipartite 3-regular graphs for $N = 6, 8, 10$. The ITE-BE layer further enhances the performance of QAOA especially for large graphs.